Mon. Not. R. astr. Soc. (1979) **189**, 897–906

Emission band and continuum photometry of Comet West (1975n) – I. Heliocentric dependence of the flux in the emission bands and the continuum

K. R. Sivaraman, G. S. D. Babu, M. K. V. Bappu and M. Parthasarathy *Indian Institute of Astrophysics, Bangalore-560 034, India*

Received 1979 June 17; in original form 1979 April 5

Summary. Spectrum scans of the coma of Comet West (1975n) covering the range λλ 3700–5700 Å were made on eight nights when the heliocentric distance of the comet varied from 0.588 to 0.853 AU. These have been used to derive the absolute flux in the CN (0, 0), C_3(4050), C_2(1, 0) and C_2(0, 0) bands as well as in the continuum. Enhancements in the band emissions were noticed on three nights in CN(0, 0), C_3(4050) and C_2(1, 0). The column densities of neutral sodium atoms are derived from scans around 5900 Å on four nights. The column densities of CO^+ ions corresponding to four prominent band sequences are evaluated from two scans of the tail.

1 Introduction

Spectrophotometry of the emission bands and continua of comets form an important source of information giving insight into the physical processes taking place in the neutral atmospheres of comets. In recent years photoelectric spectrum scans of the coma have increasingly come into use; these with medium spectral and spatial resolution have added much to our knowledge of cometary phenomena. Photoelectric photometry with narrow band filters chosen to isolate the emission bands and the neighbouring continuum (Vaný́sek 1969; Brown 1974; Kohoutek 1974; A'Hearn & Cowan 1975; A'Hearn, Thurber & Millis 1977) has the inherent disadvantage that the contamination caused by the broad transmission wings of the filter can never be estimated accurately and, therefore, remains a principal source of error in the flux estimations. Photographic plates exposed through narrow band filters have similar spectral purity limitations together with the poor precision of photographic photometry. In this context, Malaise's (1966) cometary photometer is an attempt to overcome many of these common sources of errors and keep them to a minimum. The use of Fourier transform spectrometer by A'Hearn (1975) for observing Comet Kohoutek marks a new era in cometary observations leading to very dependable determinations of the various physical parameters concerning the neutral atmospheres of comets.

We report herein the results of a study based on an extensive programme of photoelectric spectrophotometry of Comet West (1975n) carried out at the Kavalur Observatory.

2 Observations

Comet West was observed on eight nights during the post-perihelion period between 1976 March 13–24 when the heliocentric distance varied from 0.588 to 0.853 AU and the geocentric distance varied from 0.941 to 1.068 AU. The observations were obtained with the automated spectrum scanner (Bappu 1977) at the Cassegrain focus of the 102-cm reflector. The scanner was operated on four nights in the pulse counting mode and on four nights it was used in the DC mode. The image scale in the Cassegrain focal plane is 16 arcsec/mm. A circular diaphragm of 1.6 mm diameter, which corresponds to 25.9 arcsec as projected on the sky, was used on all the nights. The exit slot was kept at 10 Å in the first order during the four nights when pulse counting was done; this was changed to 20, 40 and 50 Å width in the second order while operating in the DC mode and on the last night of our observations on March 24, the exit slot was at 50 Å in the first order. On each night, before the comet observations were commenced, two standard stars, θ Crt and 58 Aql, were scanned to provide the nightly extinction values and the system calibration. The flux values adopted

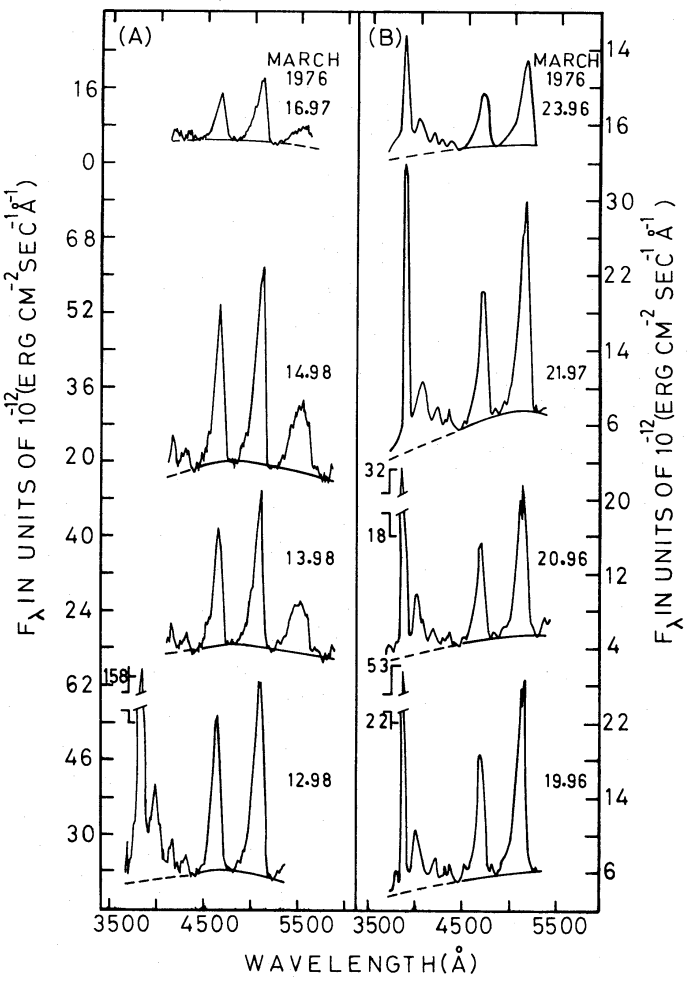

Figure 1. Absolute flux distribution in the head of Comet West seen through a diaphragm of 25.9 arcsec diameter. The epoch of the observations are given in U.T. The curves in Box A are those from the on-line computer and the curves in box B from the dc mode scans.

for these stars are those of Hayes & Latham (1975). The sky brightness was measured immediately preceding and following the cometary scans. After correcting for this background sky brightness, which was not of a significant level, the data were reduced to yield absolute magnitudes and absolute fluxes (F_ν). The resulting flux distribution is shown in Fig. 1, the ordinate being F_λ in units of erg cm^{-2} s^{-1} Å^{-1}. The emission band sequence of CN(0, 0) at λ 3883 Å is the strongest. The emission features of C_3 at λ 4050 Å, CN(0, 1) at λ 4216 Å, CH at λ 4280 Å and the Swan band sequences of C_2 corresponding to (2, 0) at λ 4380 Å, (1, 0) at λ 4737 Å, (0, 0) at λ 5165 Å and (0, 1) at λ 5635 Å can readily be identified. The continuum is easily located at λ 4464 Å, λ 4861 Å and λ 5263 Å; a smooth curve drawn through these locations defines the continuum in the visible region. The location of the continuum shortward of λ 4464 Å is generally not very reliable in cometary spectra due to the presence of the many rotational structures of the CN, C_3 and C_2 bands. Nevertheless, we have visually estimated the regions of continuum with the aid of the Swings and Haser Cometary Atlas. Such a continuum location is indicated by the dashed line in Fig. 1.

3 Emission band sequence flux ratios

We have measured the area under each band profile above the smoothed continuum and calculated the corresponding total flux for each band sequence for all the scans. The intensities of the band sequences relative to that of $C_2(0,0)$ band sequence at λ 5165 Å are listed in Table 1. The observed flux in the $C_2(0, 0)$ band sequence is given in the fourth column. These emission band flux ratios are comparable to those obtained for Kohoutek by Babu (1974) and by A'Hearn (1975) for the range of the heliocentric distances involved. The total number of molecules (N) of CN(0, 0) and $C_2(1, 0)$ contained in a cylinder of diameter 25.9 arcsec in the line of sight and extending through the comet, are computed using the relation of Wurm (1943),

$$N = L \frac{m_e}{\pi e^2 f \cdot p \cdot \rho(\nu, r)} \qquad (1)$$

where $L = 4\pi\Delta^2 F_\lambda$; Δ – comet–earth distance; F_λ – flux in erg cm^{-2} s^{-1} reduced to a standard area projected by the diaphragm of 25.9 arcsec diameter at Δ= 1.0 AU; f is the

Table 1. Observed fluxes of the emission bands.

Date 1976 March U.T.	r in AU	Δ in AU	★$F(C_2, 5165)$ (erg cm^{-2} s^{-1})	$F/F(C_2, 5165)$							$\frac{F(\text{cont}, 4861)}{F(C_2, 5165)}$
				CN 3883	C_3 4050	CN 4214	CH 4280	C_2 4360	C_2 4737	C_2 5636	
12.98	0.588	0.941	5.360×10^{-9}		0.402	0.087	0.012	0.051	0.696		1.664
13.98	0.611	0.953	4.122			0.075	0.010	0.067	0.641	0.570	1.659
14.98	0.633	0.967	5.195			0.074	0.011	0.096	0.688	0.613	1.586
16.97	0.684	0.992	1.746			0.084	0.030	0.061	0.566	0.510	1.260
19.96	0.756	1.027	2.250	0.788	0.318	0.084	0.026	0.032	0.751		1.120
20.96	0.782	1.038	1.897	0.862	0.324	0.061	0.022	0.053	0.610		1.202
21.97	0.809	1.047	2.783	0.761	0.362	0.109	0.032	0.040	0.589		1.078
23.97	0.853	1.068	1.223×10^{-9}	1.003	0.388	0.136	0.070	0.080	0.603		1.112

★ These fluxes are over the entire band sequence covering 400 Å.

Table 2. Column densities of molecules of CN(0, 0) and C_2(1, 0).

Date 1976 March U.T.	$N_{CN(0,0)}$	$N_{C_2(1,0)}$
12.98		11.63×10^{31}
13.98		8.89×10^{31}
14.98		12.91×10^{31}
16.97		4.17×10^{31}
19.96	0.78×10^{31}	8.71×10^{31}
20.96	0.77×10^{31}	6.38×10^{31}
21.97	1.069×10^{31}	9.67×10^{31}
23.97	0.688×10^{31}	4.83×10^{31}

oscillator strength; p is the vibrational transition probability and $\rho(v, r)$ is the solar radiation density at the given frequency and at the location of the comet. The values of f, p and $\rho(v, r)$ used in our calculations are those adopted by Kohoutek (1974). The column densities of the CN and C_2 molecules are tabulated in Table 2.

4 Flux variation

The observed fluxes were reduced to a standard geocentric distance ($\Delta = 1.0$) to study the variation with heliocentric distance r. These reduced fluxes for C_2(1, 0), C_2(0, 0) and C_3(4050) are plotted in Fig. 2. The solid line represents the least square fit $F_\lambda = F_\lambda^0 r^{-n}$ for each of the emission series. The points denoted by open circles in Fig. 2, have been omitted while working out the least squares solution. Two of these representing enhancements in the fluxes of all the emission features, simulate outbursts. The decrease in brightness of all

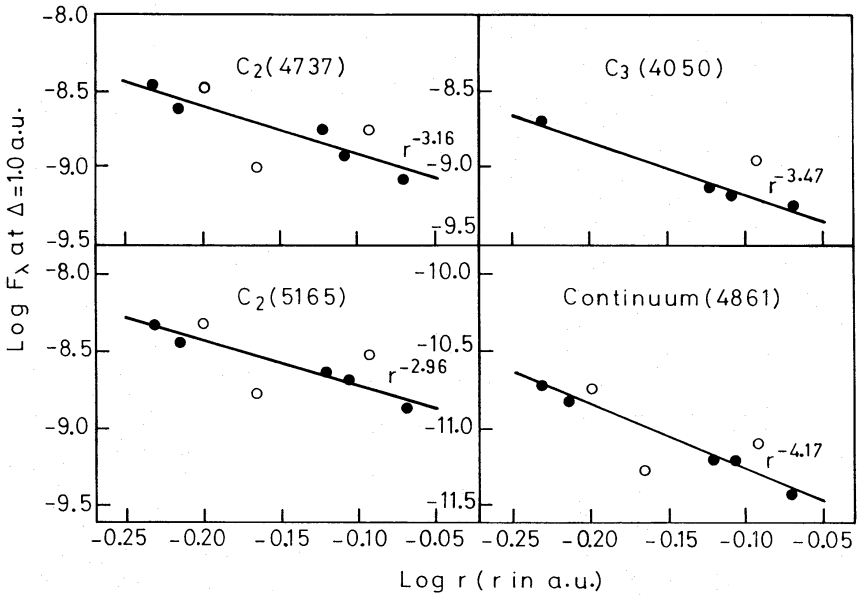

Figure 2. The reduced flux of the emission bands and the continuum of Comet West (1975a) as a function of the heliocentric distance r. The solid line represents $F_\lambda = F_\lambda^0 r^{-n}$. The values of n are shown therein. Open circles represent points associated with outbursts and have not been included for the least squares fit solution.

the features on March 16.97 is presumably a part of the oscillation of the brightness in the wake of an outburst.

Observations by A'Hearn *et al.* (1977) show similar fluctuations. They have a much larger coverage over the heliocentric distance. The variation of C_2 flux with r obtained by us and A'Hearn *et al.* matches well whereas our index for C_3 variation is higher than theirs. The difference could possibly be due to the use of a small entrance diaphragm by us ($\approx 10^4$ km at 1 AU) compared to the larger ones used by A'Hearn *et al.* A part of the decrease in the C_3 flux noticed in our data is due to the increase in the scale length of the parent molecules of C_3 rather than an actual decrease of the emitters themselves. But since scale lengths of C_3 and their parent molecules are inadequately known, it would be premature at the present time to attempt to isolate the contribution of the above process towards the slope of the C_3 emission flux.

It is seen that the fluxes in these emission bands vary approximately as r^{-3} in the heliocentric distance interval $r = 0.588$ to 0.853 AU. Now this decrease is a function of R, the solar flux available to the comet, $s(p)$ the scale length of the parent molecule and $s(d)$ the scale length of C_2 and C_3 molecules and A their abundances. This can be symbolically represented as

$$f(R, s(d), s(p), A) = r^{-3}. \tag{2}$$

Now, R varies as r^{-2} and the abundance A varies as r^{-1} as seen from a plot of the column density of C_2 molecules from Table 2. The observations of Delsemme & Moreau (1973) of Comet Bennett show that the scale length of the C_2 molecules varies as r^2. Their range of heliocentric distances is nearly the same as ours. If we assume the same r^2 law to hold good for Comet West too, then we find from equation (2) that the scale length of the parent molecule should simulate an r^{-2} variation, as against the proportional law that is weakly indicated from their observations. Since the demand that the scale length of the parent molecule should follow an r^{-2} variation will conflict with the concept of the increase of scale length consequent to the expansion of the coma with increase in r values, and that the observations of Delsemme & Moreau are not conclusive enough on the proportional law, we are led to believe that the decay of the parent molecule may not be related to the solar flux in a simple way as represented above and more observations on the scale length variation with r are absolutely necessary to settle this question.

5 NaI emission

The region around 5890 Å was scanned separately on four nights, to record the sodium emission. We see such emission on the scans till March 16.97. The scan of the following day does not show even a trace of emission. The last day of the visibility of sodium emission is, therefore, reckoned as March 17 at $r = 0.684$ AU. This agrees with our expected value of r for the disappearance of sodium emission (Bappu & Sivaraman 1969). The sodium emission scans were converted into absolute flux values in the same way as for the molecular emission scans. Such values reduced to standard projected area of the diaphragm (at $\Delta = 1.0$ AU) are given in Table 3. Since the emission is a resonance fluorescence phenomenon, the number of neutral atoms of sodium in the cylinder with a projected base area of 25.9 arcsec and through the comet can be computed following Wurm (1943).

Setting $p = 0.63 \times 10^8$ (Wiese, Smith & Miles 1969), $f = 1$ and $\rho(\nu, r) = 7.13 \times 10^{-20} r^{-2}$ erg cm^{-3} Hz^{-1} (Labs & Neckel 1968), the column densities were derived for the four nights of observations and are presented in Table 3.

Table 3. Sodium (NaI) emission flux and column densities.

Date 1976 March U.T.	F(NaI, 5893) (erg cm^{-2} s^{-1})	N(NaI)
11.99	315.6×10^{-12}	6.6×10^{19}
13.99	69.2×10^{-12}	1.8×10^{19}
14.99	185.1×10^{-12}	5.4×10^{19}
16.99	62.9×10^{-12}	2.2×10^{19}

6 Continuum energy distribution

The brightness of the continuum is seen to fall very rapidly with heliocentric distance (Fig. 2). The ratio of continuum brightness to the $C_2(0, 0)$ emission fell from 1.664 to 1.112 during our observing spell (Table 1). From a comparison of similar data on Comets Kohoutek and Bennett (Babu 1974; Babu & Saxena 1972) we find that Comet West was as dusty as Comet Kohoutek was in its pre-perihelion phase, but less dusty than what Comet Bennett was during its post-perihelion phase.

In order to compare the nightly variation of the continuum energy distribution in the coma, we have normalized the absolute magnitudes of the continuum at 4464 Å. Fig. 3 is a plot of these continuum absolute magnitudes. The phase angle of scattering ϕ for each of these nights is indicated on each curve. The progressive reddening with decrease in phase angle is obvious. This is about 0.4 mag for a variation of phase angle from 60 to 80° (see inset of Fig. 3). Surprisingly, Neff & Ketelsen (1976) from a low resolution photoelectric

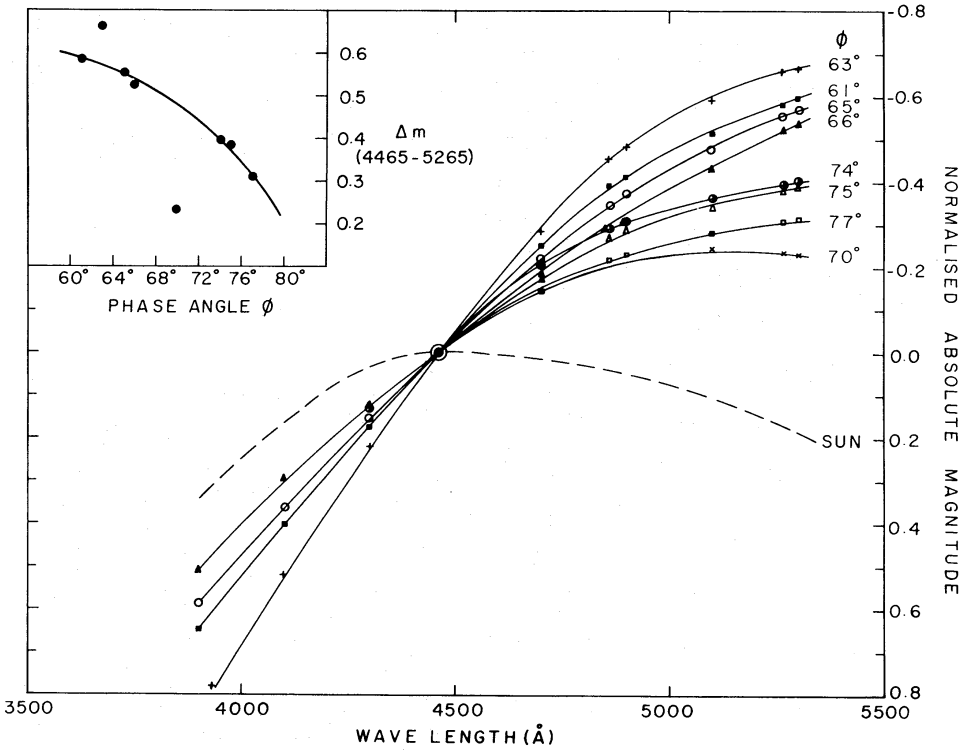

Figure 3. Continuum energy distribution curves of Comet West at various phase angles ϕ. The inset shows the progressive decrease in the colour index Δm (4465–5265 Å) with increasing ϕ. Phase angle 61° corresponds to March 23.97 and 77° corresponds to March 12.98.

spectrophotometric study conclude that the continuum does not exhibit any phase angle dependence. This, at least partly, may be the outcome of their use of low resolution techniques.

7 Spectrum of the tail

We have obtained tail scans covering the range λλ 3500–5000 Å on March 12.01 and March 15.00, with the entrance aperture located at 255 arcsec and 70 arcsec respectively away from the nucleus in the E–W direction into the tail and with an exit slot of 5 Å. The high resolution is sufficient to bring out some of the details of the features in the spectrum of the tail. A plot of the absolute fluxes is given in Figs 4 and 5. On March 12.01, the emission bands due to $CO^+(1, 0)$ at λ 4544 Å, $CO^+(2, 0)$ at λ 4251 Å, $CO^+(3, 0)$ at λ 4013 Å and $CO^+(4, 0)$ at λ 3803 Å are quite prominent, besides many other bands due to N_2^+, CH^+, C_3 head etc. The CN(0, 0) emission even at 1.04×10^5 km is stronger than any of the CO^+ band emissions. On March 15.00, with the scan location relatively nearer the nucleus, all the CO^+ features are seen along with an obviously enhanced CN(0, 0) emission. The band systems have been identified from Greenstein's (1962) table of wavelengths of Comet Humason (1961e). These wavelengths are marked in Figs 4 and 5 to enable identification of

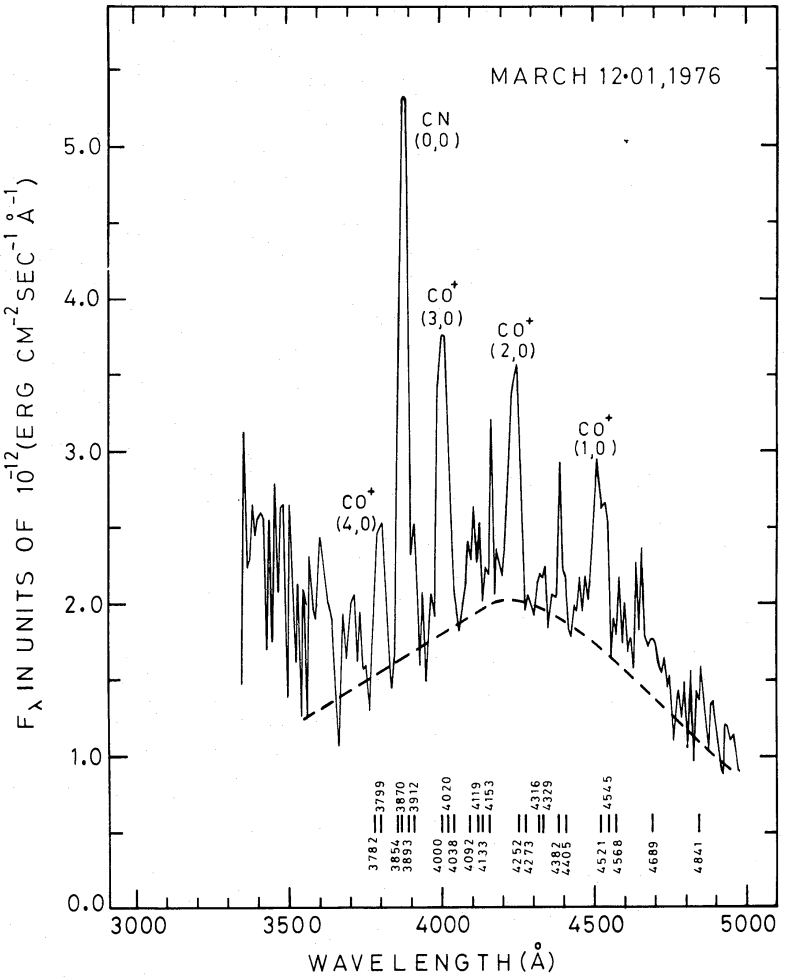

Figure 4. Absolute flux distribution in the tail of Comet West on 1976 March 12.01, seen through an entrance diaphragm 25.9 arcsec diameter located at 255 arcsec away from nucleus in the E–W direction. Identification wavelengths are from Greenstein (1962).

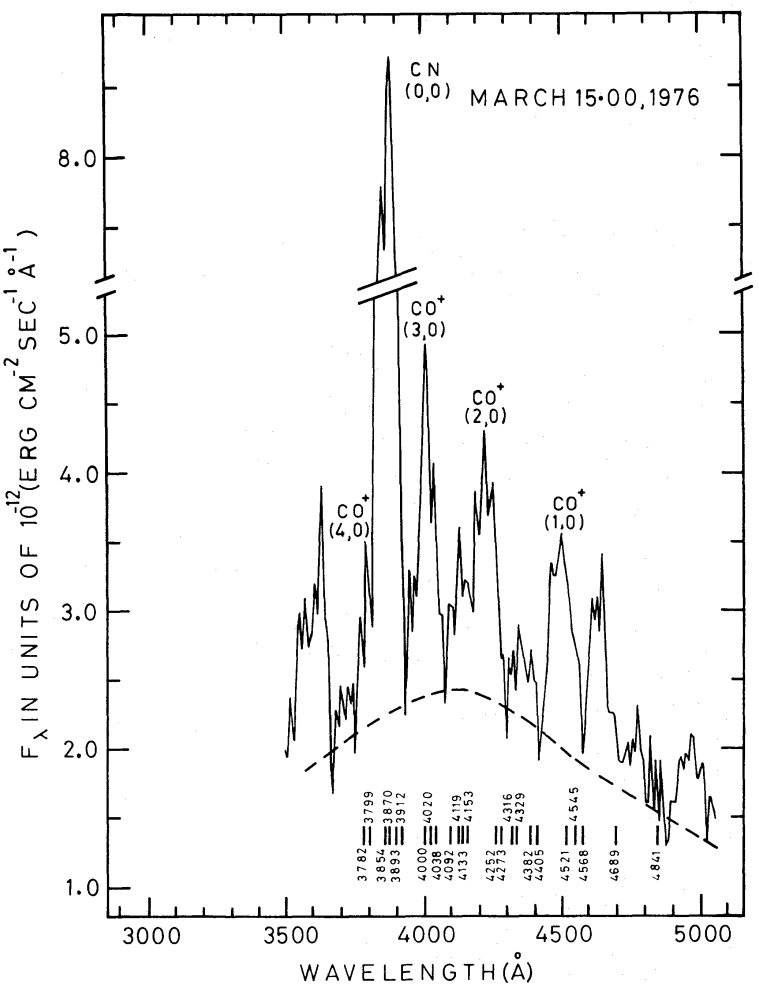

Figure 5. Absolute flux distribution in the tail of Comet West on 1976 March 15.00, through an entrance diaphragm of 25.9 arcsec diameter, located at 70 arcsec away from the nucleus in the E–W direction. Identification wavelengths are from Greenstein (1962).

the strongest features. Fluxes in the tail for each band are given in Table 4. To calculate the total number of CO^+ ions in the line of sight corresponding to each of the transitions (v', v'') using the formula of Wurm (1943), we have adopted the value of 0.0056 for the oscillator strength, f, (Arpigny 1965) and the smoothed relative vibrational transition probabilities of Robinson & Nicholls (1960). These are also given in Table 4. The values of $\rho(v, r)$ the solar radiation density at the location of the comet are computed for the four wavelengths of our interest using the mean intensity values given by Labs & Neckel (1968). The resulting column densities (N) are also set out in Table 4, along with the ratios N_{CO^+}/N_{CN}.

Such estimates of the CO^+ ion abundances in cometary tails are available only for Comet Bester and Comet Humason. The abundance determination by Arpigny (1965) shows that the ratio N_{CO^+}/N_{CN} is 0.5 for Comet Bester (1947k) and nearly 750 for Comet Humason (1961e). Our values for this ratio differ considerably from those of either of the above mentioned comets. The radiation around λ 3883 Å, contains contributions from CO_2^+, N_2^+, OH^+ at wavelengths 3854, 3870, 3893, 3912 Å intricately mixed with that from CN(0, 0) sequence. This makes the ratio N_{CO^+}/N_{CN} less meaningful, particularly as an index to compare the activity in the tail of different comets.

Table 4. Emission flux and column densities of CO^+ in the tail of Comet West.

Transition (v', v'')	Transition probability p	March 12.01 (ρ = 255 arcsec)			March 15.00 (ρ = 70 arcsec)		
		$F(CO^+)$	$N(CO^+)$	$\frac{N(CO^+)}{N(CN)}$	$F(CO^+)$	$N(CO^+)$	$\frac{N(CO^+)}{N(CN)}$
$CO^+(4,0)$	0.16	38.5×10^{-12}	2.34×10^{30}	8.73	38.9×10^{-12}	3.29×10^{30}	2.74
$CO^+(3,0)$	0.23	86.6×10^{-12}	2.01×10^{30}	7.51	113.4×10^{-12}	3.66×10^{30}	3.05
$CO^+(2,0)$	0.25	49.5×10^{-12}	1.03×10^{30}	3.86	78.5×10^{-12}	2.29×10^{30}	1.90
$CO^+(1,0)$	0.18	36.9×10^{-12}	0.75×10^{30}	2.78	27.7×10^{-12}	0.78×10^{30}	0.65

8 Conclusion

The measured emission fluxes show that the $C_2(1, 0)$ emission falls off as $r^{-3.16}$, $C_2(0, 0)$ as $r^{-2.96}$, $C_3(4050)$ as $r^{-3.47}$. The continuum follows a $r^{-4.17}$ variation. The total number of molecules of CN(0, 0) and $C_2(1, 0)$ contained in the cylinder (see Table 2) and the strong continuum shows that the comet exhibited a larger gaseous as well as dust output compared to some of the comets of the recent past.

The column densities corresponding to four of the emission band sequences of CO^+ ions and of CN(0, 0) band are computed from the spectrum scans of the tail. Similar data are very scanty in the literature and so a comparison is not possible. It is, therefore, necessary to accumulate observations of this type for more comets to obtain a better insight into the mechanism of CO^+ ion production and behaviour in the tail.

References

A'Hearn, M. F., 1975. *Astr. J.*, **80**, 861.
A'Hearn, M. F. & Cowan, J. J., 1975. *Astr. J.*, **80**, 852.
A'Hearn, M. F., Thurber, C. H. & Millis, R. L., 1977. *Astr. J.*, **82**, 518.
Arpigny, C., 1965. *Mem. Acad. R. Belgique*, **35**, Part 5, Liege Contr. No. 493.
Babu, G. S. D., 1974. *IAU Coll.* No. 25, *The Study of Comets*, p. 220, GSFC, Greenbelt, Maryland.
Babu, G. S. D. & Saxena, P. P., 1972. *Bull. astr. Insts Czech.*, **23**, 346.
Bappu, M. K. V., 1977. *Kodaikanal Obs. Bull. Ser. A*, **2**, 64.
Bappu, M. K. V. & Sivaraman, K. R., 1969. *Solar Phys.*, **10**, 496.
Brown, L. W., 1974. *IAU Coll.* No. 25, *The Study of Comets*, p. 70, GSFC, Greenbelt, Maryland.
Delsemme, A. H. & Moreau, J. L., 1973. *Astrophys. Lett.*, **14**, 181.
Greenstein, J., 1962. *Astrophys. J.*, **136**, 688.
Hayes, D. S. & Latham, D. W., 1975. *Astrophys. J.*, **197**, 593.
Kohoutek, L., 1974. *IAU Coll.* No. 25, *The Study of Comets*, p. 50, GSFC, Greenbelt, Maryland.
Labs, D. & Neckel, H., 1968. *Z. Astrophys.*, **69**, 1.
Malaise, D., 1966. *Nature et Origine des Cometes*, 13th Liege Symp., p. 199.
Neff, J. S. & Ketelsen, D. A., 1976. *Trans. IAU, Proc. Sixteenth General Assembly, Grenoble 1976*, Vol. XVI B, p. 138.
Robinson, D. & Nicholls, R. W., 1960. *Proc. phys. Soc. Lond. A*, **75**, 817.
Vanýsek, V., 1969. *Bull. astr. Insts Czech.*, **20**, 355.
Wiese, W. L., Smith, M. W. & Miles, B. M., 1969. *Atomic Transition Probabilities Vol. II, Sodium Through Calcium*, US Dept. of Commerce, National Bureau of Standards.
Wurm, K., 1943. *Mitt. Hamburg. Sternw.*, **8**, No. 51.